Journal of the Serbian Chemical Society
JSCS-info@shd.org.rs • www.shd.org.rs/JSCS

ACCEPTED MANUSCRIPT

Please cite this article as N. Ž. Prlainović, M. P. Rančić, I. Stojiljković, J. B. Nikolić, S. Ž. Drmanić, I. Ajaj, A. D. Marinković, *J. Serb. Chem. Soc.* (2018), https://doi.org/10.2298/JSC170408003P

J. Serb. Chem. Soc. 83 (0) 1–17 (2018)
JSCS–4962

UDC
Original scientific paper

Experimental and theoretical study on solvent and substituent effect in 3-(4-substituted)phenylamino)isobenzofuran-1(3*H*)-ones

NEVENA Ž. PRLAINOVIĆ[1#], MILICA P. RANČIĆ[2#], IVANA STOJILJKOVIĆ[2], JASMINA B. NIKOLIĆ[3*#], SAŠA Ž. DRMANIĆ[3#], ISMAIL AJAJ[4] and ALEKSANDAR D. MARINKOVIĆ[3#]

[1]*InnovationCenter, Faculty of Technology and Metallurgy, Karnegijeva 4, 11120 Belgrade, Serbia,* [2]*Faculty of Forestry, University of Belgrade, KnezaVišeslava 1, 11030 Belgrade, Serbia,* [3]*Faculty of Technology and Metallurgy, University of Belgrade, Karnegijeva 4, 11120 Belgrade, Serbia and* [4]*Faculty of Arts and Science, The university of El-margeb, Mesallata, Libya*

(Received 8 April, revised 28 November, accepted 7 December 2017)

Abstract: The substituent and solvent effect on solvatochromism in3-((4-substituted)phenylamino)isobenzofuran-1(3*H*)-ones were studied using experimental and theoretical methodology. The effect of specific and non-specific solvent–solute interactions on the UV-Vis absorption maxima shifts were evaluated by using the Kamlet-Taft and Catalán solvent parameter sets. The experimental results were studied by DFT and TD-DFT methods. The HOMO/LUMO energies (E_{HOMO}/E_{LUMO}) and energy gap (E_{gap}) values, as well as the mechanism of electronic excitations and the changes in the electron density distribution in both ground and excited states of the investigated molecules were studied by the calculation in the gas phase. The electronic excitations were calculated by TD-DFT method in solvent methanol. It was found that both substituents and solvents influence the degree of π-electron conjugation of the synthesized molecules and affect the intramolecular charge transfer character.

Keywords: phthalides; solvatochromism; substituent effect; LSER; quantum chemical calculation.

INTRODUCTION

Phthalides or 3*H*-isobenzofuran-1-ones represent a widespread group of secondary metabolites in plants, responsible for numerous pharmacological properties and biological activities. To date, all known natural phthalide compounds have been identified as derivatives of 3H-isobenzofuran-1-one.[1] Phthalides are characterized by a bicyclic core (Scheme 1), derived from the

* Corresponding author. E-mail: jasmina@tmf.bg.ac.rs
# Serbian Chemical Society member.
https://doi.org/10.2298/JSC170408003P

fusion of a γ-lactone with benzene. They are considered internal esters of the corresponding γ-hydroxy carboxylic acids. Although the occurrence of the parent phthalide (3*H*-isobenzofuran-1-one) in natural products dates back to the 18th century, the interest for a wide range of biological activities of its diverse derivatives has only recently arisen in the scientific community.[2]

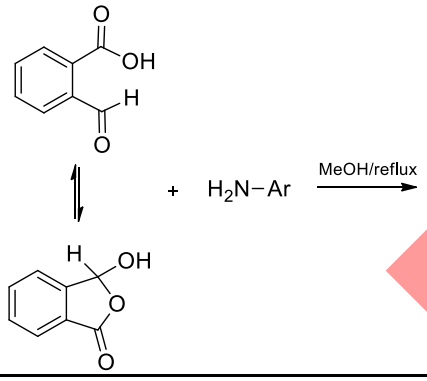

Compound	-Ar	Compound	-Ar
1	Phenyl	**6**	4-Chloro phenyl
2	4-Methyl phenyl	**7**	4-Acetyl phenyl
3	4-Methoxy phenyl	**8**	4-Nitro phenyl
4	4-Hydroxy phenyl	**9**	2-Pyridyl
5	4-Fluoro phenyl	**10**	3-Pyridyl

Scheme 1. General procedure for synthesis of 3-((4-substituted)phenylamino)isobenzofuran-1(3*H*)-ones.

Phthalide are also versatile starting materials and key intermediates for the synthesis of a variety of natural products.[3] For example, 3-arylphthalides are intermediates for the synthesis of tri- and tetracyclic natural products such as anthracycline antibiotics.[2] Various chemical modifications of this heterocycle have resulted in compounds with a wide spectrum of biological activities *e.g.*, antibacterial,[4] antitubercular,[5] antifungal,[6] anti-HIV,[7] antioxidant,[8] antitumor and immunosuppressive activity.[9] Although phthalides are components of traditional medicines from ancient times, the diverse range of their therapeutic activities has only recently attracted the attention of scientists.[2] The success of *n*-butylphthalide (NBP),[3] which is currently in the market as an antiplatelet drug for ischemia-cerebral apoplexy, has led to the development of phthalides as a class of pharmaceutically important natural products. It has also been approved, by the state food and drug administration of China in 2002, as an anti-ischemic stroke drug. It inhibits platelet aggregation, improves microcirculation, and mitigates ischemic brain injury.[2] However, most of the recent studies have dealt with 3-substituted phthalides due to their wide range of pharmacological applications.

Up to date, the studies on the structure and activity relationships have been limited toNBP.[3]

However, the previous literature data indicate that several molecular properties, particularly electronic properties, usually correlate with their biological activity, so it can be noted that the future prospects for design and development of new biologically active molecules are based on the correlation between theoretical and experimental properties. The photophysical properties of molecules are mainly governed by the polarity of the medium, hydrogen bonding and electronic substituent effects.[10,11]

In the present work, a series of 3-((4-substituted)phenylamino)isobenzofuran-1(3*H*)-ones was synthesized in order to study the influence of the solvent–solute interactions on the shifts in UV spectra. Interactions with the solvent were investigated by the use of linear solvation energy relationships (LSER). The effects of solvent dipolarity/polarizability and solvent–solute hydrogen bonding interactions were evaluated by means of the LSER model of Kamlet-Taft Eq. (1):[12,13]

$$\nu_{\max} = \nu_{o} + s\pi^{*} + b\beta + a\alpha \quad (1)$$

where ν_{max} is the absorption maxima frequency positions, π^* is an index of the solvent dipolarity/polarizability; β is a measure of the solvent hydrogen-bond acceptor (HBA) basicity; α is a measure of the solvent hydrogen-bond donor (HBD) acidity, and ν_o is the maximum position value in cyclohexane as reference solvent. The regression coefficients *s*, *b* and *a* in Eq. (1) measure the relative susceptibilities of the absorption frequencies to the solvent effect.

The effects of solvent dipolarity, polarizability and solvent–solute hydrogen bonding interactions were evaluated by means of the linear solvation energy relationship (LSER) model of Catalán,[14] given by Eq. (2):

$$\nu_{\max} = \nu_{o} + a\mathrm{SA} + b\mathrm{SB} + c\mathrm{SP} + d\mathrm{SdP} \quad (2)$$

where SA, SB, SP and SdP characterize solvent acidity, basicity, polarizability and dipolarity of a solvent, respectively; and *a* to *d* are the regression coefficients describing the sensitivity of the absorption maximum to different types of the solvent–solute interactions. The separation of non-specific solvent effects, term π^* in Eq. (1), into two terms: dipolarity and polarizability, SP and SdP in Eq. (2), contributes to advantageous analysis of the solvatochromism of the studied compounds. The solvent parameters used in Eq. (1) are given in Tables S-I and S-II of the Supplementary material to this paper.

Physico-chemical properties of 3-((4-substituted)phenylamino)isobenzofuran-1(3*H*)-ones (Scheme 1) have been investigated by using both experimental and theoretical methodology. The computational studies include geometry optimization by density functional theory calculations (DFT) and time-dependent density functional theory calculations (TD-DFT) of electronic transitions.[15]

EXPERIMENTAL

Materials

All chemicals used in this study were reagent grade or p.a. quality, and used as received. Phthalaldehyde acid, aniline, glacial acetic acid, aniline, 4-methylaniline, 4-methoxyaniline, 4-hydroxyaniline, 4-fluoroaniline, 4-chloroaniline, 4-nitroaniline, 4-acetylaniline, 2-aminopyridine and 3-aminopyridine were purchased from Sigma Aldrich. All used solvents were of spectroscopic quality (Table S-I).

General procedure for synthesis of 3-((4-substituted)phenylamino)isobenzofuran-1(3H)-ones

A solution of 5mmol of the aniline or aniline derivatives in 10 ml methanol was refluxed with phthalaldehydic acid (0.75 g, 5mmol) for 3 hours in presence of few drops of acetic acid. The product obtained was collected by filtration, air dried and recrystallized from solvent ethanol. The structures and the numbering of the synthesized compounds are given in Table S-III of the Supplementary material.

Characterization methods

The ^{1}H and ^{13}C NMR spectral measurements were done on a Varian Gemini 200 spectrometer. The spectra were recorded at room temperature in deuterated dimethylsulphoxide (DMSO-d_6) at ambient temperature. The chemical shifts are expressed in ppm values referenced to TMS (δ_H=0 ppm) in ^{1}H NMR spectra, and the residual solvent signal (δ_C=39.5 ppm) in ^{13}C NMR spectra. FT-IR spectra were recorded on Nicolet iS10 Spectrometer (Thermo Scientific) using ATR. Elemental analysis (C, H, N and O) was performed using a VARIO EL III Elemental analyzer, and F, and Cl content was calculated as subtraction.

The UV absorption spectra were measured in the range 200-600 nm using Shimadzu 1700 UV/Vis spectrophotometer. The UV/Vis spectra were taken in spectroscopic quality solvents (Fluka) at the concentration of 1×10^{-5} mol dm^{-3}. Three measurements were performed and mean value was presented.

Theoretical calculations

Geometries of all molecular species were optimized by DFT method using B3LYP/6-31G(d,2p)basis set. In order to find the global minimum on the potential energy surface, multiple geometry optimizations were performed for every compound, with varying rotatable torsion angle(θ, Scheme 1) for increment of 30° and minimizing the energy with respect to all geometrical parameters. The nature of the lowest energy minimum was further confirmed with frequency calculations; no negative frequency was found.

Theoretical absorption spectra and ground/excited state properties are calculated on DFT/B3LYP/6-31G(d,2p)optimized geometries using TD-DFT. The TD-DFT calculations were done in solvent methanol with CAM-B3LYP long range corrected functional[15]and 6-31G(d,p) basis set. Solvent in TD-DFT calculations was simulated with Polarizable Continuum model (PCM). All quantum chemical calculations were carried out using Gaussian09 program package.[16]

RESULTS AND DISCUSSION

Spectral properties of 3-sustituted-5-arylidene-2,4-thiazolidinediones

Phthalaldehydic acid is often represented as having an aldehyde and acid group. However, on the basis of spectroscopic data, it is obvious that, depending

on the solvent and temperature, phthalaldehydic acid exists in both, open and ring form structure.[20] The open and ring form structures are presented in the Scheme 1. The reaction of phthalaldehydic acid with aniline was described previously.[21] The 3-anilino phthalide was the only product obtained by refluxing the reaction mixture for 3 hours in methanol as a solvent.

The study of the solvent effects on the absorption spectra of organic compound allows access to some fundamental molecular properties.[12,17,18] One of the general concepts, concerning the relationship between molecular structure and absorption spectrum, leads to conclusion that the existence of planarity in molecular geometry produces higher bathochromic shift in UV-Vis spectra due to increased π-conjugation throughout investigated molecules.[19] In order to study the influence of the solvent–solute interactions on the absorption maxima, the UV-Vis spectra of ten synthesized 3-((4-substituted)phenylamino)isobenzofuran-1(3*H*)-ones has been recorded in sixteen solvents of different properties. The characteristic spectra in dichloromethane and methanol are shown as examples in Fig. 1. From the presented UV-Vis spectra (Fig. 1), a diversity of the spectra with two main bands could be noticed. First band appears in the range from 215-225 nm, and the other in the range from 275-285 nm with the exception of compound **8** that appears at 330 nm. It could be observed that both position and intensity of main absorption bands, presented in Tables I and II, depend on the electronic structure of compounds and solvent properties. The data from Tables I and II indicate that values of absorption frequencies of the investigated compounds depend on the substituent and solvent effect, though the absorption bands of both electron-donor and electron-acceptor substituted derivatives appear at similar wavelengths (in the range 10–20 nm) compared to unsubstituted compound **1**.

From the results of the absorption maxima presented in the Table I it can be concluded that the first peak of 3-((4-substituted)phenylamino)isobenzofuran-1(3*H*)-ones is less sensitive to the substituent electronic effects and medium properties, though most of the electron-acceptor substituents (acetyl, nitro, fluoro, 2-pyridyl) induce hypsochromic shift, when compared to the unsubstituted compound in all solvents. The introduction of electron-donor substituent into the arylidene part produces mostly bathochromic shift except in some solvents such as butanol, ethanol, ethane-1,2-diol, dioxolane and tetrahydrofuran.

The absorption maxima of the second peak positioned at longer wavelengths of 3-((4-substituted)phenylamino)isobenzofuran-1(3*H*)-ones (Table II) showed batochromic shift, compared to the unsubstituted compound **1** in all solvents. The introduction of electron-donor substituents into the arylidene part produces larger batochromic shifts, suggesting a more pronounced ICT interaction in a molecule. On the other hand, the absorption maxima of 3-((4-substituted)phenylamino)isobenzofuran-1(3*H*)-ones derivatives showed hypsochromic shift for all substances, and the largest was found for *nitro* substituted derivative **(8)**.

TABLE I. Absorption frequencies ($\nu_{max}\times10^{-3}$/ cm^{-1}) of 3-((4-substituted)phenylamino)isobenzofuran-1(3*H*)-ones in selected solvents for the lower wavelength peak

Solvent	Substituent									
	1	**2**	**3**	**4**	**5**	**6**	**7**	**8**	**9**	**10**
1,2-Dichloroethane	42.92	41.67	42.92	42.92	43.10	43.86	43.86	41.15	44.25	42.74
Decan-1-ol	42.74	42.74	42.37	42.92	43.10	48.78	43.20	42.70	44.05	42.74
Dichloromethane	42.92	42.74	42.92	43.20	43.20	43.29	43.48	42.91	43.48	42.74
1,4-Dioxane	42.28	42.92	42.19	42.92	43.01	43.48	43.29	40.98	43.10	42.83
Ethane-1,2-diol	42.19	42.37	43.29	42.74	42.55	43.67	42.92	40.16	43.48	42.74
Ethanol	42.74	42.92	42.74	43.10	43.29	44.25	43.86	41.15	44.05	42.55
Water	43.48	42.64	42.92	42.37	43.53	44.37	43.83	40.98	43.67	42.92
Hexane	43.38	43.29	42.74	42.84	43.48	44.64	44.64	41.49	44.64	43.48
2-Methyl propan-1-ol	42.74	42.64	42.92	42.83	43.10	44.25	43.86	41.07	43.96	42.64
Propan-2-ol	43.10	42.92	42.92	43.10	43.29	44.25	44.05	42.55	44.05	42.55
Methanol	42.92	42.74	42.92	42.92	44.44	43.29	44.05	40.98	44.05	42.55
Butan-1-ol	43.01	42.92	42.83	43.48	43.29	43.86	43.20	42.37	44.05	42.74
Propan-1-ol	42.92	42.74	41.67	43.29	43.29	44.64	44.44	41.32	44.05	42.55
Butan-2-ol	42.92	42.92	42.92	43.29	43.29	44.44	44.05	42.55	44.05	42.74
2-Methyl propan-2-ol	42.92	42.74	42.37	42.83	43.29	44.25	43.96	40.82	43.96	42.64
Tetrahydrofuran	41.67	41.67	42.92	41.75	41.84	42.49	42.50	40.98	42.02	41.67

TABLE II. Absorption frequencies ($\nu_{max}\times10^{-3}$/ cm^{-1}) of 3-((4-substituted)phenylamino)isobenzofuran-1(3*H*)-ones in selected solvents for the higher wavelength peak

Solvent	Substituent									
	1	**2**	**3**	**4**	**5**	**6**	**7**	**8**	**9**	**10**
1,2-Dichloroethane	35.71	34.48	33.44	27.47	35.71	35.64	34.25	29.76	35.59	34.60
Decan-1-ol	35.97	35.97	32.89	33.61	35.71	32.63	32.41	29.41	35.46	35.84
Dichloromethane	35.84	35.65	33.67	34.48	35.71	35.71	34.36	30.03	35.59	35.59
1,4-Dioxane	35.97	35.84	34.01	33.11	35.78	34.31	34.07	29.24	35.59	34.60
Ethane-1,2-diol	35.46	35.46	33.44	34.59	35.40	33.50	31.75	27.06	32.47	35.40
Ethanol	36.76	35.71	33.44	35.71	35.59	33.90	33.00	28.82	35.46	34.13
Water	35.52	34.36	33.44	33.78	34.42	34.13	32.52	27.97	34.36	34.36
Hexane	36.10	36.07	33.44	35.34	34.25	34.07	34.78	31.20	35.84	35.21
2-Methyl propan-1-ol	35.91	35.91	33.61	33.44	35.91	34.25	32.95	29.24	35.59	34.42
Propan-2-ol	35.71	35.59	33.56	35.71	35.59	34.36	33.00	29.41	35.40	34.13
Methanol	35.84	35.71	33.44	33.44	35.84	33.67	33.22	29.07	35.46	34.13
Butan-1-ol	35.65	35.59	33.56	35.59	34.07	33.90	31.70	27.25	35.46	35.52
Propan-1-ol	35.59	34.13	33.44	35.59	35.53	33.56	32.89	29.07	35.46	34.13
Butan-2-ol	35.71	35.71	33.44	35.71	35.71	33.90	33.00	29.07	35.46	34.25
2-Methyl propan-2-ol	35.97	35.91	32.89	33.73	35.97	35.91	33.11	29.07	35.52	34.25
Tetrahydrofuran	34.48	34.36	33.67	33.44	34.25	34.25	33.84	29.24	34.36	34.19

The photophysical properties of molecules strongly depend on the molecular geometry, which can be observed as a result of the interplay of two factors: the stabilization of a molecule by the decoupling between donor and acceptor parts

upon their twisting, and the resonance interaction leading to the planarization of the molecule.[12] Both factors can be further influenced by the polarity of the solvent. In addition, the role of steric hindrances must be taken into account. The influence of the solvent on the absorption spectra is of particular importance since it is known that spectral behaviour of an organic molecule is strongly related to its electronic structure in both ground and excited state.[12] The positions, intensities, and shapes of the absorption bands change as a result of physical intermolecular solute–solvent interaction forces (ion-dipole, dipole-dipole, dipole-induced dipole, hydrogen bonding, etc.), which primarily tend to alter the energy difference between ground and excited state of the absorbing species, containing the chromophore. Generally, the theories of solvent effects on absorption spectra assume that the chemical states of the isolated and solvated molecules are the same, and these effects are the consequence only as a physical perturbation of the relevant molecular states of the chromophores. Actually, a change of solvent is accompanied by a variation of polarity, dielectric constant or polarizability of the surrounding medium, thus influencing the solvent interactions with ground and excited state of the molecule.[12] The bathochromic shift (positive solvatochromism) is associated with the increased solvent polarity, and it is caused by the significant difference in charge distributions between the ground and excited state. The interaction of polar solvents is stronger with a more polar excited state. Therefore, more polar excited state of a molecule is more stabilized in such a case, which leads to lower absorption energies, *i.e.* to larger bathochromic shift.

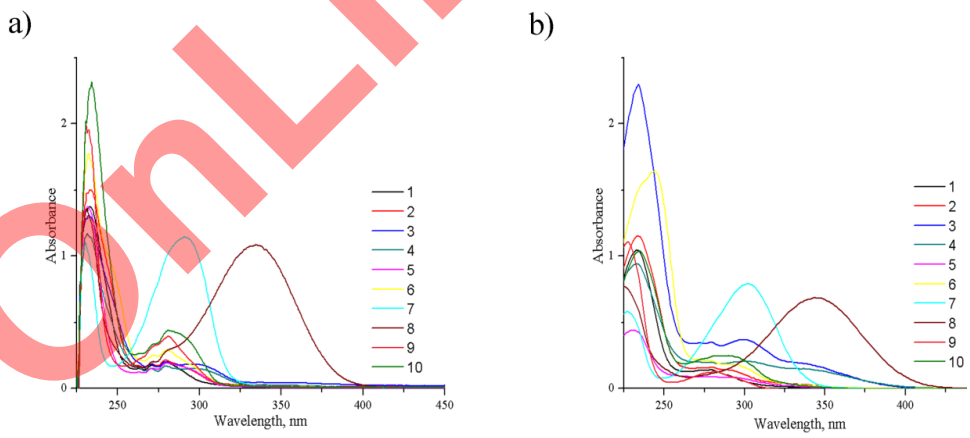

Fig. 1. Absorption spectra of compounds **1**–**10** in solvent a) dichloromethane and b) methanol.

Solvent effects on the UV–Vis absorption spectra: correlation with multi-parameter solvent polarity scales (LSER analysis)

The effect of various types of solvent–solute interactions on the absorption maxima shifts in sixteen solvents was also interpreted by means of Kamlet-Taft and Catalán LSER models.[12,13,14] The LSER method was carried out using the solvent parameters (Table SI and SII) as independent variables and absorption frequency as dependant variable. The correlation analysis was carried out using Microsoft Excel software at confidence level of 95%. The goodness of fit is discussed using the correlation coefficient (*R*), the standard error of the estimate (*sd*), and Fisher's significance test (*F*). The regression values v_0, *s*, *a*, and *b*(Kamlet-Taft),and *c*, *d*,*a*, and *b* (Catalán) fit, at the 95% confidence level, are presented in Tables S-IV and S-V and Tables S-VI and S-VII, respectively.

Results in Tables S-IV, S-V, S-VI and S-VII indicate that solvent effects on UV–Vis spectra are complex due to great diversity of both solvent and substituent effects. It can be noticed, from the results given in Tables SIV and SV that in most cases non-specific solvent effect is a factor of the highest contribution to UV-Vis spectral shifts. The negative sign of coefficient *s* for the most compounds, except coefficient *s* for the first peak in compound **4** (Table S-IV) and for the second peak in compounds **3, 5, 6, 7, 9** and **10** (Table S-V), indicates batochromic (red) shift with increasing solvent dipolarity/polarizability. This suggests better stabilization of the excited electronic state relative to ground state with increasing solvent polarity. The highest absolute values of coefficient *s* were found for compounds **6** and **8** for the lower wavelength peak and for compound **6** for the higher wavelength peak, which suggests better stabilization of the ground state relative to the excited state.

Results of the quantitative separation of the non-specific solvent effect into polarizability and dipolarity term (coefficients *c* and *d*) performed by using Catalán equation, eq. (2), are given in Tables S-VI and S-VII.

The results obtained by the use of Catalán equation provide better understanding of attractive/repulsive solvent/solute interactions and enables estimation of their appropriate contribution to ν_{max} shift in UV-Vis spectra. Comparison of the correlation results from Tables S-IV and S-V with corresponding results from Tables S-VI and S-VII revealed that in most cases correlation coefficients are more reliable for Catalán scale which highlights the importance of solvent polarizability (except for compound **6** that gave poor correlation by Catalán method with the exclusion of even 11 solvents). The correlation results, obtained according to eq. (2) (Tables S-VI and S-VII), imply that the solvent polarizability is the principal factor influencing the shift of v_{max}, whereas solvent dipolarity, acidity and basicity have moderate to low contribution. Negative values of the coefficient *c*, except for compounds **4** and **8** for the first peak and compound **10** for the second peak, indicate higher

contribution of the polarizability effect to stabilization of the excited state. Since phthalide moiety acts as an electron-accepting group, the introduction of the substituents of different electronic properties causes variation in the mobility of the π-electrons, and thus, wide range of coefficient *c* values were found. Effect of solvent dipolarity, assigned with *d* term, is of lower significance and showed complex behaviour, with the highest relative contribution for compounds **1** and **4**. Higher contribution of the solvent dipolar effect, in compounds with substituent displaying low/moderate effect, could be due to balanced contribution of two opposite effects, *i.e.*, two distinct π-electronic entities: the arylidene and phthalide moieties which cause separation of charges by creation of dipolar structure differently oriented in space.

Specific solvent–solute interactions realized through hydrogen bonding, *i.e.* HBD effect can be attributed mainly to the carbonyl group of the phthalide moiety, lactone oxygen atom and nitrogen, while solvent basicity HBA arises from amino NH group. Negative values of the coefficient *a* found in both peaks, except for compounds **2**, **4**, **6**, **8** and **10** indicate moderate to low contribution of the solvent acidity to the stabilization of the excited state.

Geometry optimization and TD-DFT calculations. Nature of the frontier molecular orbitals

The correlation results (Tables S-IV-S-VII) reflect different transmission modes of electronic substituent effect. In that context, it was necessary to optimize the geometries of the investigated molecules. 3-((4-Substituted)phenylamino)isobenzofuran-1(3H)-ones were fully optimized by the use of DFT method. The atoms numbering and results of energies of optimized molecules by the DFT/B3LYP/6-31G(d,p) method are presented in Tables S-III and S-VIII, respectively, while the optimized structures in gas phase are given in Fig. 2. Elements of the optimized geometries of investigated compounds obtained are given in Table III. It was also found that the lactone product is more stable compared to open imine structure, given in Fig S-1, for approximately 14.7 kcal/mol. In addition, the geometry of the investigated compounds was also calculated using MP2 method and the results are presented in Table S-IX.

It can be seen that geometric features of the studied 3-((4-substituted)phenylamino)isobenzofuran-1(3H)-ones follow the similar trend related to geometry parameter change *versus* substituent effect. Taking into account torsional angle (θ, Scheme 1), its change indicates that introduction of either strong electron-donating (*methoxy* or *hydroxy*) or electron-accepting substituent (*acetyl*, *nitro* or *2-pyridyl*) increases the θ values, *i.e.* increases deviation from planarity. In general, torsional angle (θ) change (83.44°) is the most pronounced when 2-pyridyl group is present in the molecule. The deviation from the planarity increases with increasing electron-acceptor ability of the arylidene substituent. From the

results in Table III, the introduction of electron-accepting substituent induces increasing of **C1'-C2'**, **C3-N** and **C1-O2** bond lengths, while oppositely, **N-C1'**, **C3-O2**, **C1=O**, **C1-C7a** and **N-H** bond lengths decreases compared to unsubstituted molecule **1**.The opposite trend is exhibited when electron-donating substituent is present. A strong electron-accepting substituent supports an electron density shift to the phenyl ring from the rest of the molecule. Greater extent of the *n,π*-delocalization causes decrease in the **N-C1'** bond length, this part of the molecule acts as a separate unit. On the contrary, in the electron-donor substituted derivatives the bond length of **N-C1'**, **N-H, C3-O2**, **C1=O** and **C1-C7a** are slightly longer, while length of **C1'-C2'**, **C3-N** and **C1-O2** bonds decrease compared to unsubstituted one giving rise to greater contribution of electron delocalization from the phthalide unit. Also, the results of the molecule geometry optimization calculated using MP2/6-31G(d,p) method, given in the Table SIX, are in agreement with the results obtained using DFT method.

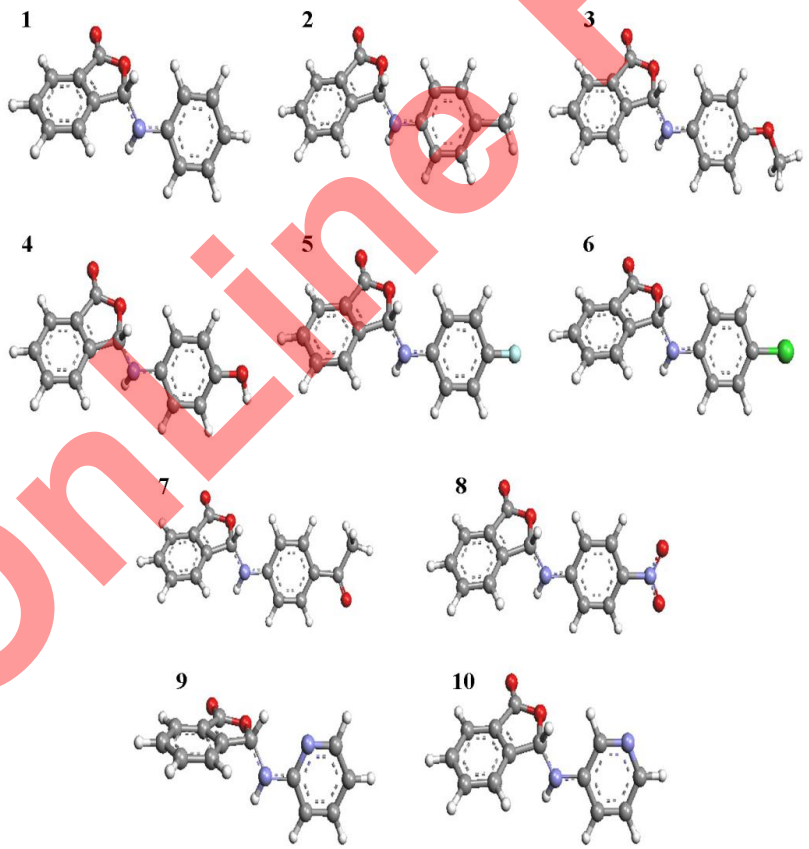

Fig. 2. Optimized structures of 3-((4-substituted)phenylamino)isobenzofuran-1(3*H*)-ones obtained using DFT method.

TABLE III. Elements of the optimized geometries of investigated compounds, 3-((4-substituted)phenylamino)isobenzofuran-1(3H)-ones 1-10 (Å) calculated by DFT/6-31G(d,p) method

Cmpd.	C1-C7a	C1=O	C1-O2	C3-O2	C3-N	N-H	N-C1'	C1'-C2'	θ / °	μ / D
1	1.4847	1.2057	1.3716	1.4777	1.4139	1.0115	1.4090	1.4047	69.86	4.804
2	1.4848	1.2059	1.3711	1.4793	1.4132	1.0117	1.4111	1.4042	69.62	4.688
3	1.4848	1.2060	1.3707	1.4820	1.4122	1.0121	1.4168	1.3989	69.92	5.476
4	1.4847	1.2060	1.3709	1.4818	1.4126	1.0123	1.4176	1.4011	69.75	5.668
5	1.4844	1.2054	1.3725	1.4777	1.4144	1.0119	1.4124	1.4045	69.16	5.358
6	1.4843	1.2050	1.3736	1.4744	1.4160	1.0115	1.4068	1.4046	69.12	5.867
7	1.4841	1.2046	1.3747	1.4703	1.4180	1.0110	1.3974	1.4092	70.14	5.724
8	1.4837	1.2036	1.3777	1.4648	1.4218	1.0108	1.3915	1.4103	70.31	8.799
9	1.4840	1.2060	1.3722	1.4693	1.4240	1.0111	1.3963	1.4084	83.44	5.139
10	1.4844	1.2048	1.3741	1.4719	1.4182	1.0120	1.4042	1.4022	69.53	6.500

The frontier molecular orbitals (FMOs) play an important role in the optical and electric properties. The HOMO represents the ability to donate an electron and LUMO to obtain an electron; the HOMO-LUMO energy gap also determines the chemical reactivity and optical polarizability of a molecule. The frontier molecular orbital energies and energy gap between HOMO and LUMO orbitals of all compounds are also calculated at the same level of theory and they are used to study the changes in the overall electronic distribution in ground and excited states of the investigated molecules in gas phase and results are presented in Table IV. The plots of the molecular calculated HOMO and LUMO molecular orbitals are presented in Table S-X. It can be noticed that electron density of HOMO orbitals for all molecules is mainly spread over the substituted phenyl ring, while electron density for the LUMO orbitals is localized on the phthalide moiety. It can also be noted that electron density of LUMO orbital for *nitro* substituted molecule is considerably high on the phenyl ring, due to strong electron accepting character of the *nitro* substituent causing the π-electron density shift to arylidene moiety, regardless of the oppositely oriented, but weaker electron-accepting character of the phthalide moiety. Generally, E_{gap} values were lower for molecules with electron-donor substituents and higher for compounds with electron-acceptor substituted molecules (except *nitro* substituted compound **8**) in comparison to unsubstituted molecule **1**. Higher energy gap in gas phase, found for the electron-acceptor substituted compounds (**7**, **9** and **10**) is a consequence of a significant HOMO orbitals stabilization. Considering the results of geometry optimization from Table III, it is clear that these are compounds with more pronounced deviation from planarity. Besides, as it can be seen in Table IV, the calculated HOMO and LUMO energies in methanol are slightly lower than in gas phase. The lowest energy gap in gas phase was observed for molecule with *methoxy* substituent (**3**) and the highest for compound containing *2-pyridyl* group (**9**) in both, gas phase and solvent methanol.

TABLE IV. Calculated energies of the HOMO and LUMO orbitals and energy gaps for investigated compounds **1**-**10**by TD-DFT/6-31G(d,p) method in gas phase and solvent methanol

Molecule	E_{HOMO} / eV	E_{LUMO}/ eV	Egap/ eV	E_{HOMO}/ eV	E_{LUMO}/ eV	Egap / eV
	Gas			Methanol		
1	–5.811	–1.439	4.372	–6.105	–1.709	4.396
2	–5.643	–1.407	4.236	–5.934	–1.699	4.235
3	–5.354	–1.375	3.979	–5.678	–1.690	3.988
4	–5.426	–1.391	4.036	–5.714	–1.690	4.024
5	–5.840	–1.499	4.341	–6.098	–1.718	4.380
6	–5.928	–1.563	4.365	–6.157	–1.735	4.422
7	–6.081	–1.625	4.456	–6.305	–1.759	4.546
8	–6.521	–2.150	4.371	–6.590	–2.604	3.986
9	–6.104	–1.327	4.777	–6.326	–1.685	4.641
10	–6.132	–1.547	4.584	–6.362	–1.742	4.620

In order to have a better understanding on the energetic behaviour of molecules, the additional TD-DFT calculations including solvent influence were done in solvent methanol with CAM-B3LYP long range corrected functional[15] and 6-31G(d,p) basis set. Solvent in TD-DFT calculations was simulated with Polarizable Continuum model (PCM). TD-DFT provides a good benchmark in the determination of spectroscopic properties due to the accurate description of ground and excited potential energy surfaces. The calculated vertical excitation energies, oscillator strength (*f*) and the composition of the most significant singlet excited states are shown in Table V. The presented results for electronic transitions also indicate that compounds show bathochromic shift compared to unsubstituted compounds in solvent methanol (except **5** and **9**), and the lowest frequency is observed for *nitro* substituted compound. These results are consistent with experimental ones (Table II). Furthermore, it is evident that only the absorption for the compound **8** originates from pure HOMO-LUMO transition (98.1%), while for the rest of the compounds other transitions are included, *e.g.* HOMO→LUMO+3 for compounds **1**, **2**, **3**, **4**, **6**, **9** and **10,** HOMO-3→LUMO for compound **5** and HOMO→LUMO+1 for compound **7**. Molecular orbital surfaces of orbitals included in the electronic transitions and their energies in solvent methanol for all compounds are presented in Fig. 3.

Comparing the calculated TD-DFT results to the experimental ones in Table VI for methanol, it is obvious that there is a good agreement of calculated with experimental values. From experimental and calculated absorption frequency results in methanol, it can be concluded that *nitro* substituted compound **8** showed the most pronounced bathochromic effect with respect to the unsubstituted compound **1**. Besides, the calculated frequencies are somewhat higher compared to the corresponding experimental values, but it is already

known in the literature that this method overestimates the energies of electronic transitions.[22]

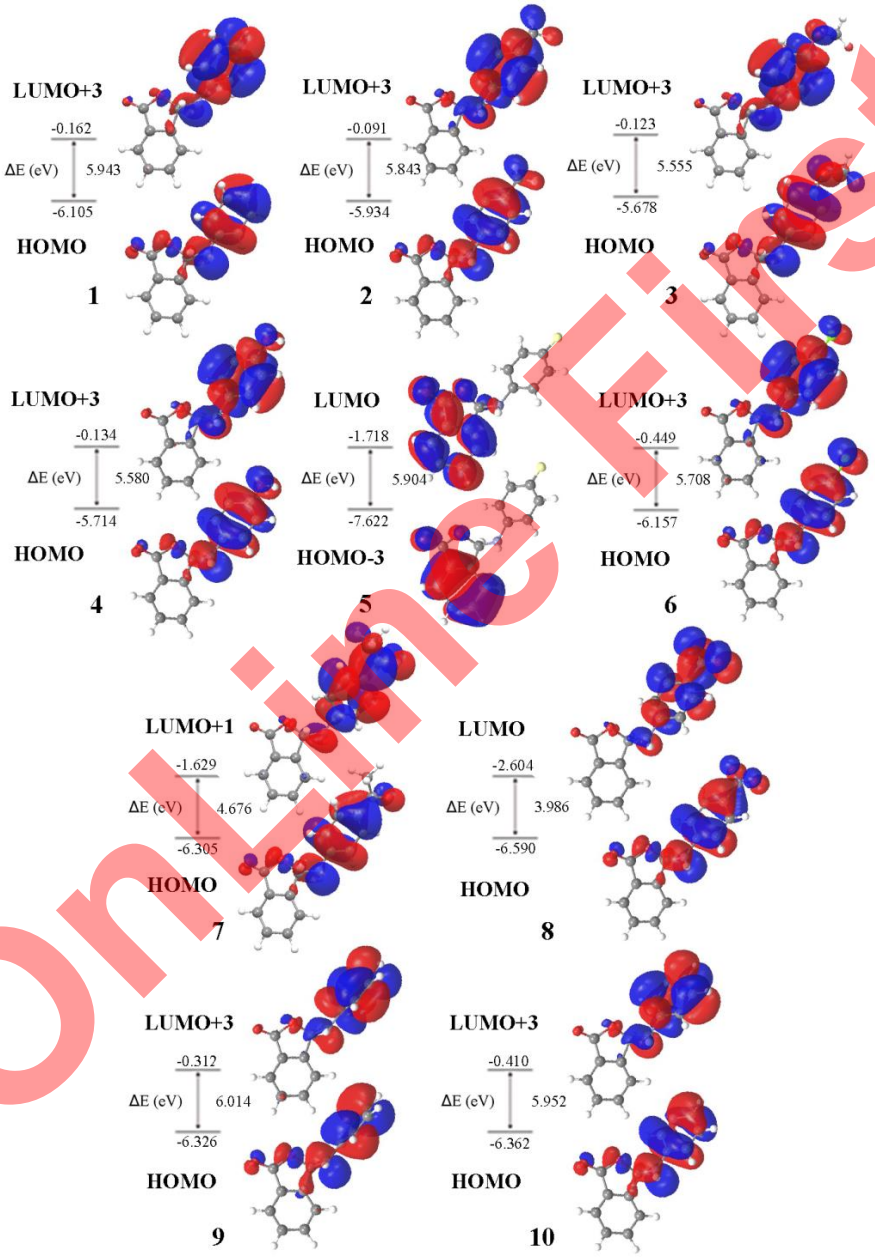

Fig. 3. The main transitions and corresponding orbitals for compounds **1**–**10** calculated by TD-DFT method in solvent methanol.

TABLE V. Calculated excitation energies (eV), oscillator strengths (*f*), CI expansion coefficient and percentage of single particle excitation contribution for the most significant singlet excited states for compounds **1-10** calculated with TD-DFT method in solvent methanol

Comp.	Excitation energy, eV	Oscillator strength	Excitation	CI expansion coefficient	Single particle excitation contribution, %
1	5.4640	0.4417	HOMO → LUMO+3	0.52237	54.6
			HOMO-3 → LUMO	-0.40185	32.3
			HOMO-1 → LUMO+2	0.14225	4.05
2	5.3915	0.5588	HOMO → LUMO+3	0.65413	85.6
			HOMO-1 → LUMO+2	-0.17583	6.2
			HOMO-3 → LUMO	0.14079	4.0
3	5.3529	0.5687	HOMO → LUMO+3	0.65988	87.1
			HOMO-1 → LUMO+2	0.16845	5.7
			HOMO-3 → LUMO	-0.10535	2.2
4	5.4258	0.4955	HOMO → LUMO+3	0.63097	79.6
			HOMO-3 → LUMO	0.20609	8.5
			HOMO-1 → LUMO+2	-0.17098	5.8
5	5.4795	0.2973	HOMO-3 → LUMO	0.58891	69.4
			HOMO → LUMO+3	0.28121	15.8
			HOMO-2 → LUMO+1	-0.17924	6.4
			HOMO-2 → LUMO	0.10049	2.0
6	5.2732	0.4984	HOMO → LUMO+3	0.61157	74.8
			HOMO-1 → LUMO	-0.25540	13.0
			HOMO-1 → LUMO+2	-0.13776	3.8
			HOMO-2 → LUMO	0.13393	3.6
7	4.3448	0.6927	HOMO → LUMO+1	0.69485	96.6
8	3.6795	0.5252	HOMO → LUMO	0.70047	98.1
9	5.5950	0.3675	HOMO → LUMO+3	0.62228	77.4
			HOMO-1 → LUMO+3	0.17793	6.3
			HOMO-2 → LUMO	-0.16060	5.2
			HOMO-5 → LUMO+1	0.12682	3.2
			HOMO-3 → LUMO+2	0.10946	2.4
10	5.4044	0.3091	HOMO → LUMO+3	0.55575	61.8
			HOMO-1 → LUMO+3	-0.35925	25.8
			HOMO-3 → LUMO	0.15478	4.8
			HOMO-4 → LUMO+1	0.10941	2.4

The experimental and theoretical study indicate that the solvatochromic and physico-chemical properties of studied phthalides are the consequence of the overall effect of the molecule geometry, influenced by the electronic substituent effects transmitted through π-conjugated systems and results obtained in this study help in assessing the potential application of the investigated compounds. Such results could be useful in designing new biologically active compounds allowing the estimation of the site of electrophilic or nucleophilic attacks in some photochemical reactions. Obtained results can also be significant in QSAR or QSPR studies in evaluation of their biological activity.

TABLE VI. Experimental and calculated absorption frequencies by TD-DFT method in solvent methanol

Molecule	$\nu_{1calc}\times10^{-3}$ / cm^{-1}	$\nu_{1exp}\times10^{-3}$ / cm^{-1}	$\nu_{2calc}\times10^{-3}$/ cm^{-1}	$\nu_{2exp}\times10^{-3}$ / cm^{-1}
1	44.07	42.92	39.39	35.84
2	43.49	42.74	38.50	35.71
3	43.17	42.92	36.44	33.44
4	43.76	42.92	36.63	33.44
5	44.19	44.44	38.04	35.84
6	42.53	43.29	36.82	33.67
7	43.61	44.05	35.04	33.22
8	39.76	40.98	29.68	29.07
9	45.13	44.05	37.82	35.46
10	43.59	42.55	37.36	34.13

CONCLUSIONS

The substituent and solvent effects on the UV-Vis absorption maxima shifts of 3-((4-substituted)phenylamino)isobenzofuran-1(3*H*)-ones were successfully evaluated, based on the experimental data and theoretical calculations. The results showed that absorption maxima are more dependent on substituent than on solvent effect. Solvent polarizability is the principal factor that influences the shift of the absorption maxima, whereas the solvent dipolarity, acidity and basicity are of lower importance. The absorption maxima undergo the bathochromic shift with the increasing solvent polarizability indicating that the excited state is more polarizable than the ground state. Specific interactions through hydrogen bonding, expressed by the solvent acidity and basicity, can be attributed mainly to the *carbonyl* and *amino* moiety, and it is slightly affected by the substituent present in the arylidene part.

The optimized geometries of investigated compounds showed that introduction of either strong electron-donating (*methoxy* or *hydroxy*), or electron-accepting substituent (*acetyl*, *nitro* or *2-pyridyl*) increases the θ values, *i.e.* increases the deviation from planarity. In general, the torsion angle (θ) change (83.44º) is the most pronounced when *2-pyridyl* group is present in the molecule.

Generally, in comparison with unsubstituted molecule **1,** E_{gap} values were lower for molecules with electron-donating substituents and higher for compounds with electron-accepting molecules. The lowest energy gap in gas phase was observed for the compound with *methoxy* substituent (**3**) and the highest for the compound containing *2-pyridyl* group (**9**). It can be noticed that the electron densities of the HOMO orbitals for all molecules are dominantly populated on the substituted phenyl ring, while the electron density for the LUMO orbitals are populated on the phthalide moiety (except for *nitro* substituted compound). However, it is evident from TD-DFT results that only the absorption for the compound **8** originates from pure HOMO-LUMO transition (98.1%), while for the rest of the compounds other transitions are included, *e.g.*

HOMO→LUMO+3**,** HOMO-3→LUMO or HOMO→LUMO+1. Results of TD-DFT calculations, in methanol as a solvent, showed a good agreement of calculated and experimental frequencies.

SUPPLEMENTARY MATERIAL

Solvent parameters and results of characterization are available electronically at the pages of journal website: http://www.shd.org.rs/JSCS/, or from the corresponding author on request.

Acknowledgement. This work was supported by the Ministry of Education, Science and Technological Development of Serbia (Project Number 172013).

ИЗВОД

ЕКСПЕРИМЕНТАЛНО И ТЕОРИЈСКО ПРОУЧАВАЊЕ УТИЦАЈА РАСТВАРАЧА И СУПСТИТУЕНАТА КОД 3-(4-СУПСТИТУИСАНИХ)ФЕНИЛАМИНО)ИЗО-БЕНЗОФУРАН-1(3*H*)-ОНА

НЕВЕНА ПРЛАИНОВИЋ[1], МИЛИЦА РАНЧИЋ[2], ИВАНА СТОЈИЉКОВИЋ[2], ЈАСМИНА НИКОЛИЋ[3], САША ДРМАНИЋ[3], ИСМАИЛ АЈАЈ[4] и АЛЕКСАНДАР МАРИНКОВИЋ[3]

[1]*Иновациони центар Технолошко–металуршког факултета, Универзитет у Београду, Карнегијева 4, 11120 Београд,* [2]*Шумарски факултет, Универзитет у Београду, Кнеза Вишеслава 1, 11030 Београд,* [3]*Технолошко–металуршки факултет, Универзитет у Београду, Карнегијева 4, 11120 Београд и* [4]*Faculty of Arts and Science, The university of El-Margeb, Mesallata, Libya*

Утицај супституената и растварача на солватохромизам код 3-(4-супституисаних)-фениламино)изобензофуран-1(3H)-она је проучаван експерименталном и теоријском методологијом. Утицај специфичних и неспецифичних интеракција између молекула растварача и испитиваних једињења на померања UV-Vis апсорпционих максимума су процењени помоћу једначина Камлет-Тафта и Каталана. Експериментални резултати су тумачени помоћу DFT и TD-DFT метода. HOMO/LUMOенергије (E_{HOMO}/E_{LUMO}), њихове разлике (E_{gap}),као и механизам побуђивања електона и промене расподеле електронске густине и у основном и у побуђеном стању испитиваних једињења,проучаван је израчунавањем у гасној фази. Електронски прелази су израчунати TD-DFT методом у метанолу као растварачу. Утврђено је да и супституенти и растварачи утичу на промену електронске густине, тј. на величину коњугације и на унутармолекулску промену наелектрисања.

(Примљено 8. априла, ревидирано 28. новембра, прихваћено 7. децембра 2017)

REFERENCES

1. G. Lin, S. S.-K. Chan, H.-S. Chung, S.-L. Li, *Stud. Nat. Prod. Chem.***32** (2005) 611
2. R. Karmakar, P. Pahari, D. Mal, *Chem. Rev.* **114** (2014) 6213
3. Y.-Q.Zhu, J.-X. Li, T.-F.Han, J.-L. He,K. Zhu, *Eur. J. Org. Chem.* **2017** (2017) 806
4. T. Saito, T. Itabashi, D. Wakana, H, Takeda, T. Yaguchi, K. Kawai, T. Hosoe, *J. Antibiot.* **69** (2016) 89
5. R. A. Limaye, V. B. Kumbhar, A. D. Natu, M. V. Paradkar, V. S. Honmore, R. R. Chauhan, S. P. Gample, D. Sarkar, *Bioorg. Med. Chem. Lett* .**23** (2013) 711
6. G. Strobel, E. Ford, J. Worapong, J. K. Harper, A. M. Arif, D. M. Grant, P. C. W. Fung, R. M. W. Chau, *Phytochemistry* **60** (2002) 179
7. S.F. Brady, M.M. Wagenaar, M.P. Sing, J.E. Janso, *Org. Lett.* **2** (2000) 4043

8. T. H. Chou, I. S. Chen, T. L. Hwang, T. C. Wang, T. H. Lee, L. Y. Cheng, Y. C. Chang, J. Y. J. Y. Cho, J. J. Chen, *J. Nat. Prod.*, **71** (2008) 1692
9. L. P. L. Logrado, C. O. Santos, L. A. S. Romeiro, A. M. Costa, J. R. O. Ferreira, B. C. Cavalcanti, O. M. de Moraes, L. V. Costa-Lotufo, C. Pessoa, M. L. dos Santos, *Eur. J. Med. Chem.* **45** (2010) 3480
10. M.Rančić,N. Trišović, M. Milčić, G. Uščumlić, A. Marinković,*Spectrochim. Acta A* **86** (2012)500
11. A. Sarkar, P. Banerjee, S. U. Hossain, S. Bhattacharya, S. C. Bhattacharya, *Spectrochim. Acta A* **72** (2009) 1097
12. C.Reichardt, *Solvents and Solvent Effects in Organic Chemistry,3rd, Updated and Enlarged Edition*, Wiley-VCH, Weinheim, Germany, 2003, p. 432
13. M. J. Kamlet, J. L. M. Abbound, R. W. Taft, *An examination of linear solvation energy relationships*,in*Progress in Physical Organic Chemistry*,vol. 13, R.W. Taft, Ed(s).,Wiley, New York, USA, 1981, p. 485
14. J. Catalán, *J. Phys. Chem. B* **113** (2009) 5951
15. T. Yanai, D. Tew, N. Handy,*Chem. Phys. Lett.* **393** (2004) 51
16. *Gaussian 09, Revision C.01*, Gaussian Inc., 2009, Wallingford, CT
17. M. S. Masoud, R. M. I. Elsamra, S. S. Hemdan, *J. Serb. Chem. Soc.* **82** (2017), doi: 10.2298/JSC170204032M
18. M. Faraji, A. Farajtabar, *J. Serb. Chem. Soc.* **81** (2016) 1161
19. D. R. Brkić, J. B. Nikolić, A. R. Božić, V. D. Nikolić, A. D. Marinković, H. Elshaflu, S. Ž. Drmanić, *J. Serb. Chem. Soc.* **81** (2016) 979
20. A. Amer, H. Zimmer, *J. Heterocyclic Chem.* **18** (1981) 1625
21. S. N. Khattab, S. Y. Hassan, A. El-Faham, A. M. M. El Massry, A. Amer, *J. Heterocyclic Chem.* **44** (2007) 617
22. D. Jacquemin, A. Planchat, C. Adamo, B. Mennucci, *J. Chem. Theory Comput.*, **8** (2012) 2359.

Journal of the Serbian Chemical Society
JSCS@tmf.bg.ac.rs • www.shd.org.rs/JSCS
J. Serb. Chem. Soc. *83* (0) S1–S12 (2018) *Supplementary material*

SUPPLEMENTARY MATERIAL TO

Experimental and theoretical study on solvent and substituent effect in 3-(4-substituted)phenylamino)isobenzofuran-1(3*H*)-ones

NEVENA Ž. PRLAINOVIĆ[1#], MILICA P. RANČIĆ[2#], IVANA STOJILJKOVIĆ[2], JASMINA B. NIKOLIĆ[3*#], SAŠA Ž. DRMANIĆ[3#], ISMAIL AJAJ[4] and ALEKSANDAR D. MARINKOVIĆ[3#]

[1]InnovationCenter, Faculty of Technology and Metallurgy, Karnegijeva 4, 11120 Belgrade, Serbia, [2]Faculty of Forestry, University of Belgrade, KnezaVišeslava 1, 11030 Belgrade, Serbia, [3]Faculty of Technology and Metallurgy, University of Belgrade, Karnegijeva 4, 11120 Belgrade, Serbia and [4]Faculty of Arts and Science, The university of El-margeb, Mesallata, Libya

J. Serb. Chem. Soc. *83* (0) (2018) 000–000

TABLE S-I. Solvent parameters used in Kamlet–Taft equation[1,2]

Solvent	π	β	α
1,2-Dichloroethane	0.81	0.10	0.00
Decan-1-ol	0.45	0.82	0.70
Dichloromethane	0.82	0.10	0.13
1,4-Dioxane	0.27	0.49	0.00
Ethane-1,2-diol	0.9	0.52	0.90
Ethanol	0.54	0.75	0.86
Water	1.09	0.47	1.17
Hexane	0.00	0.00	-0.04
2-Methyl propan-1-ol	0.40	0.84	0.79
Propan-2-ol	0.48	0.84	0.76
Methanol	0.60	0.66	0.98
Butan-1-ol	0.47	0.84	0.84
Propan-1-ol	0.52	0.90	0.84
Butan-2-ol	0.40	0.80	0.69
2-Methyl propan-2-ol	0.41	0.93	0.41
Tetrahydrofuran	0.58	0.55	0.00

* Corresponding author. E-mail: jasmina@tmf.bg.ac.rs

TABLE S-II. Solvent parameters used in Catalán equation[3]

Solvent	SP	SdP	SA	SB
1,2-Dichloroethane	0.77	0.74	0.03	0.13
Decan-1-ol	0.72	0.38	0.26	0.91
Dichloromethane	0.76	0.77	0.04	0.18
1,4-Dioxane	0.62	0.32	0.66	0.00
Ethane-1,2-diol	0.78	0.91	0.72	0.53
Ethanol	0.63	0.78	0.40	0.66
Water	0.68	0.99	1.06	0.03
Hexane	0.62	0.00	0.00	0.06
2-Methyl propan-1-ol	0.66	0.68	0.31	0.83
Propan-2-ol	0.63	0.80	0.28	0.83
Methanol	0.60	0.90	0.60	0.54
Butan-1-ol	0.67	0.65	0.34	0.80
Propan-1-ol	0.65	0.75	0.37	0.78
Butan-2-ol	0.66	0.70	0.22	0.89
2-Methyl propan-2-ol	0.63	0.73	0.16	0.93
Tetrahydrofuran	0.71	0.63	0.00	0.59

RESULTS OF THE CHARACTERIZATION

3-(phenylamino)isobenzofuran-1(3H)-one (1). Colorless needles, 0.55 g (74 %) yield, mp 179-180°C, IR (ATR): 3334m (N-H), 3038w (C-H, Ar), 1734s (C=O), 1605m (N-H), 1285w (C-N), 1206w (C-O-C), 1098m (C-O-C) cm^{-1}; 1H NMR (200 MHz, DMSO-d_6, δ): 6.54 (d, 1H, *J*=8.0 Hz, H8), 6.83 (dd, 2H, J_1=8 Hz, J_2=2 Hz, H2', H6'), 6.95-7.00 (m, 1H, H4'), 7.13 (d, *J*=8.0 Hz, H3), 7.24 (dd, 2H, J_1=8 Hz, J_2=2 Hz, H3',H5'), 7.70-7.76 (m, 2H, H5, H6), 7.84-7.92 (m, 2H, H4, H7). ^{13}C NMR (50 MHz DMSO-d_6, δ): 88.53, 114.39, 114.84, 119.84, 124.62, 125.43, 129.64, 131.04, 134.91, 145.67, 146.38, 169.70.

Elemental analysis for $C_{14}H_{11}NO_2$: Calculated. C 74.65, H 4.92, N 6.22, O 14.21; found C 74.69, H 4.91, N 6.17, O 14.23.

3-((4-methylphenyl)amino)isobenzofuran-1(3H)-one (2). Colorless needles, 0.58 g (78 %) yield, mp 183-185°C, IR (ATR): 3345m (N-H), 3020w (C-H, Ar), 1736s (C=O), 1615m (N-H), 1285m (C-N), 1218w (C-O-C), 1097m (C-O-C) cm^{-1}; 1H NMR (200 MHz, DMSO-d_6, δ): 2.23 (*s*, 3H, CH_3), 6.46 (d, 1H, *J*=8.0 Hz, H8), 6.87-7.05 (m, 4H, H2', H3', H5', H6'), 7.13 (d, 1H, *J*=8.0 Hz, H3), 7.66-7.75 (m, 2H, H5, H6), 7.81-7.91 (m, 2H, H4, H7). ^{13}C NMR (50 MHz, DMSO-d_6, δ): 169.39, 159.48, 146.15, 142.96, 134.51, 130.68, 129.78, 129.71, 128.15, 127.79, 124.87, 124.31, 114.70, 88.75, 20.33.

Elemental analysis for $C_{15}H_{13}NO_2$: Calculated. C 75.30, H 5.48, N 5.85, O 13.37; found C 75.31, H 5.48, N 5.80, O 13.41.

3-((4-methoxyphenyl)amino)isobenzofuran-1(3H)-one (3). Colorless needles, 0.64 g (83 %) yield, mp 143-144°C, IR (ATR): 3321m (N-H), 3031w (C-H, Ar), 1740s (C=O), 1597w (N-H), 1255m (C-N), 1113w (C-O-C), 1076m (C-O-C) cm^{-1}; 1H NMR (200 MHz, DMSO-d_6, δ): 3.70 (s, 3H, CH_3), 6.52 (d, 1H,

J=8.0 Hz, H8), 6.88-7.05 (m, 4H, H2', H3', H5', H6'), 7.13 (d, 1H, *J*=8.0 Hz, H3), 7.66-7.73 (m, 2H, H5, H6), 7.85-7.91 (m, 2H, H4, H7). ^{13}C NMR (50 MHz DMSO-d_6, δ): 169.34, 159.80, 153.33, 146.03, 139.19, 139.04, 134.34, 130.66, 128.05, 124.95, 124.50, 116.14, 115.06, 114.76, 89.50.

Elemental analysis for $C_{15}H_{13}NO_3$: Calculated. C 70.58, H 5.13, N 5.49, O 18.80; found C 70.51, H 5.17, N 5.51, O 18.81.

3-((4-hydroxyphenyl)amino)isobenzofuran-1(3H)-one (4). Colorless needles, 0.65 g (87 %) yield, mp 180-183°C, IR (ATR): 3352m (N-H), 3177m (O-H), 3177w (C-H, Ar), 1710s (C=O), 1616w (N-H), 1258m (C-N), 1208s (C-O-C), 1108m (C-O-C) cm^{-1}; 1H NMR (200 MHz, DMSO-d_6, δ): 6.48 (d, 1H, *J*=8.0 Hz, H8), 6.67-6.71 (m, 2H, H2', H6 '), 6.84-6.89 (m, 2H, H3', H5 '), 7.63 (d, 1H, *J*=8.0 Hz, H3), 7.66-7.90 (m, 4H, H4, H5, H6, H7). ^{13}C NMR (50 MHz, DMSO-d_6, δ) 169.30, 159.09, 151.75, 145.34, 138.13, 134.10, 130.59, 128.48, 125.66, 125.24, 124.80, 117.04, 116.21, 89.74.

Elemental analysis for $C_{14}H_{11}NO_3$: Calculated. C 69.70, H 4.60, N 5.81, O 19.90; found C 69.80, H 4.57, N 5.79, O 19.84.

3-((4-fluorophenyl)amino)isobenzofuran-1(3H)-one (5). Colorless needles, 0.59 g (79 %) yield, mp 188-189°C, IR (ATR): 3330m (N-H), 3044w (C-H, Ar), 1728s (C=O), 1610w (N-H), 1229m (C-N), 1208s (C-O-C), 1108w (C-O-C) cm^{-1}; 1H NMR (200 MHz, DMSO-d_6, δ): 6.52 (d, 1H, *J*=8.0 Hz, H8), 6.94-7.01 (m, 2H, H3', H5'), 7.05-7.09 (m, 2H, H2', H6'), 7.15 (d, 1H, *J*=8.0 Hz, H3), 7.67-7.92 (m, 4H, H4, H5, H6, H7). ^{13}C NMR (50 MHz, DMSO-d_6, δ) 169.32, 158.81, 154.14, 145.98, 141.92, 134.60, 130.77, 127.67, 124.92, 124.30, 116.00, 115.80, 115.64, 88.62.

Elemental analysis for $C_{14}H_{10}FNO_2$: Calculated. C 69.13, H 4.14, F 7.81, N 5.76, O 13.16; found C 69.01, H 4.20, F 7.76, N 5.86, O 13.17.

3-((4-chlorophenyl)amino)isobenzofuran-1(3H)-one (6). Colorless needles, 0.54 g (72 %) yield, mp 180-182°C, IR (ATR): 3341m (N-H), 3020w (C-H, Ar), 1732s (C=O), 1560m (N-H), 1303m (C-N), 1206m (C-O-C), 1090m (C-O-C) cm^{-1}; 1H NMR (200 MHz, DMSO-d_6, δ): 6.52 (*d*, 1H, *J*=8.0 Hz, H8), 6.88 (dd, 2H, J_1=8 Hz, J_2=2 Hz, H2', H6'), 7.14 (d, 1H, *J*=8.0 Hz, H3), 7.28 (dd, 2H, J_1=8 Hz, J_2=2 Hz, H3', H5'), 7.71-7.76 (m, 2H, H5, H6), 7.82-7.92 (m, 2H, H4, H7). ^{13}C NMR (50 MHz, DMSO-d_6, δ): 169.26, 159.45, 145.86, 144.47, 134.68, 130.83, 129.10, 127.55, 124.96, 124.32, 123.08, 116.09, 116.03, 87.72.

Elemental analysis for $C_{14}H_{10}ClNO_2$: Calculated. C 64.75, H 3.88, Cl 13.65, N 5.39, O 12.32; found C 64.61, H 3.74, Cl 13.69, N 5.43, O 12.53.

3-((4-acetylphenyl)amino)isobenzofuran-1(3H)-one (7). Colorless needles, 0.50 g (66 %) yield, mp 246-247°C, IR (ATR): 3340s (N-H), 3020w (C-H, Ar), 1760s (C=O), 1596s (N-H), 1284m (C-N), 1220m (C-O-C), 1107w (C-O-C) cm^{-1}; 1H NMR (200 MHz, DMSO-d_6, δ): 2.50 (s, 3H, CH_3), 6.55 (d, 1H, *J*=8.0 Hz, H8), 7.04 (dd, 2H, J_1=8 Hz, J_2=2 Hz, H2', H6 '), 7.25 (d, 1H, *J*=8.0 Hz, H3),

7.69-7.73 (m, 2H, H3', H5'), 7.85-7.95 (m, 4H, H4, H5, H6, H7). ^{13}C NMR (50 MHz DMSO-d_6, δ): 196.18, 169.18, 159.16, 150.02, 145.70, 134.81, 130.92, 130.49, 128.62, 127.35, 125.04, 124.37, 113.67, 113.56, 86.53, 26.49.

Elemental analysis for $C_{16}H_{13}NO_3$: Calculated. C 71.90, H 4.90, N 5.24, O 17.96; found C 71.93, H 4.86, N 5.28, O 17.93.

3-((4-nitrophenyl)amino)isobenzofuran-1(3H)-one (8). Colorless needles, 0.48 g (64 %) yield, mp 241-243°C, IR (ATR): 3330m (N-H), 3044w (C-H, Ar), 1728s (C=O), 1610s (N-H), 1229w (C-N), 1208m (C-O-C), 1083m (C-O-C) cm^{-1}; 1H NMR (200 MHz, DMSO-d_6, δ): 6.58 (d, 1H, *J*=8.0 Hz, H8), 7.10 (dd, 2H, J_1=8 Hz, J_2=2 Hz, H2', H6 '), 7.26 (d, 1H, *J*=8.0 Hz, H3), 7.71-7.96 (m, 4H, H4, H5, H6, H7), 8.17 (dd, 2H, H3', H5 '). ^{13}C NMR (50 MHz, DMSO-d_6, δ): 168.99, 159.69, 152.04, 145.35, 139.47, 134.94, 131.09, 127.12, 126.11, 125.14, 124.43, 113.83, 113.72, 85.70.

Elemental analysis for $C_{14}H_{10}N_2O_4$: Calculated. C 62.22, H 3.73, N 10.37, O 23.68; found C 62.18, H 3.69, N 10.40, O 23.73.

3-(2-pyridynylamino)isobenzofuran-1(3H)-one (9). Colorless needles, 0.43 g (57 %) yield, mp 206-207°C, IR (ATR): 3329w (N-H), 3040w (C-H, Ar), 1751s (C=O), 1594s (N-H), 1262s (C-N), 1225w (C-O-C), 1063s (C-O-C) cm^{-1}; 1H NMR (200 MHz, DMSO-d_6, δ): 6.92 (d, 1H, *J*=8.0 Hz, H8), 7.47 (d, 1H, *J*=8.0 Hz, H3), 7.85-7.89 (m, 1H, H4'), 7.97-8.03 (m, 2H, H5', H6'), 7.67-7.89 (m, 4H, H4, H5, H6, H7). 8.48 (dd, 1H, J_1=4 Hz, J_2=2 Hz, H3'). ^{13}C NMR (50 MHz DMSO-d_6, δ): 169.34, 161.31, 159.95, 158.60, 146.31, 134.58, 130.46, 127.46, 124.77, 124.05, 113.72, 113.60, 84.58.

Elemental analysis for $C_{13}H_{10}N_2O_2$: Calculated. C 69.02, H 4.46, N 12.38, O 14.14; found C 69.00, H 4.39, N 12.44, O 14.17.

3-(3-pyridynylamino)isobenzofuran-1(3H)-one (10). Colorless needles, 0.44 g (59 %) yield, mp 159-160°C, IR (ATR): 3329w (N-H), 3042w (C-H, Ar), 1741s (C=O), 1583m (N-H), 1285s (C-N), 1215m (C-O-C), 1094m (C-O-C) cm^{-1}; 1H NMR (200 MHz, DMSO-d_6, δ): 6.64 (d, 1H, *J*=8.0 Hz, H8), 7.18 (d, 1H, *J*=8.0 Hz, H3), 7.44-7.48 (m, 1H, H6'), 7.51-7.56 (m, 1H, H5'), 7.69-7.94 (m, 4H, H4, H5, H6, H7), 8.06 (dd, 1H, J_1=4.5 Hz, J_2=2 Hz, H2'), 8.28 (d, 1H, *J*=4 Hz, H4'). ^{13}C NMR (50 MHz DMSO-d_6, δ): 169.21, 159.94, 145.81, 141.73, 140.81, 137.28, 134.75, 130.90, 127.47, 125.01, 124.34, 120.78, 87.30.

Elemental analysis for $C_{13}H_{10}N_2O_2$: Calculated. C 69.02, H 4.46, N 12.38, O 14.14; found C 68.94, H 4.45, N 12.35, O 14.26.

TABLE S-III. Structures and numbering of synthesized 3-((4-substituted)phenylamino)-isobenzofuran-1(3H)-ones

1 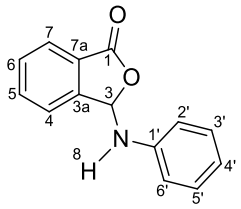	2 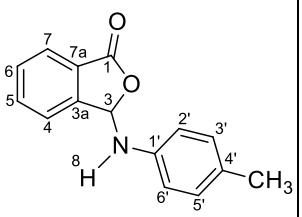	3 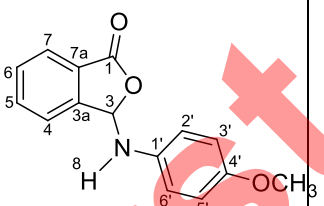
4 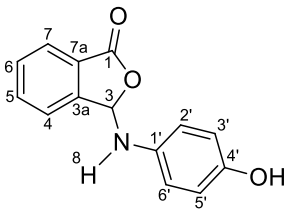	5 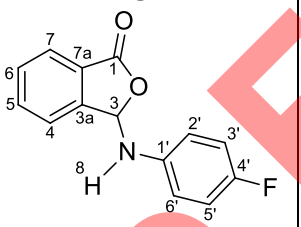	6 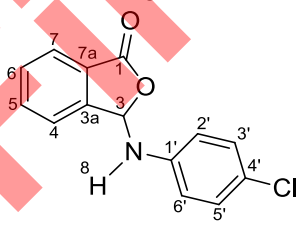
7 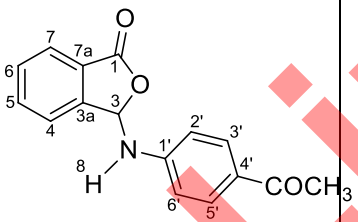	8 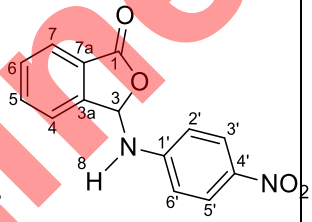	9 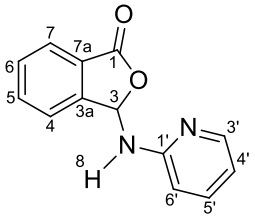
10 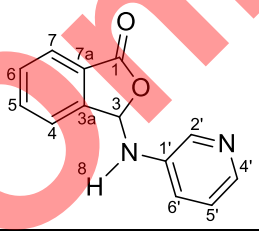		

TABLE S-IV. Results of the correlation analysis of 3-((4-substituted)phenylamino)isobenzofuran-1(3H)-ones according to Kamlet–Taft equation for the lower wavelength peak

Comp.	$\nu_0 \times 10^{-3}$ / cm^{-1}	$s \times 10^{-3}$ / cm^{-1}	$b \times 10^{-3}$ / cm^{-1}	$a \times 10^{-3}$ / cm^{-1}	R[a]	Sd[b]	F[c]	Solvent excluded from correlation
1	35.90 ±0.98	-1.71 ±0.75	-0.67 ±0.98	1.53 ±0.30	0.95	0.163	17.74	1,2-Dichloroethane, Dichloromethane, 1,4-Dioxane, Ethanol
2	43.3 ±0.19	-2.00 ±0.34	-0.46 ±0.28	1.12 ±0.24	0.91	0.18	13.57	1,2-Dichloroethane, Dichloromethane, 1,4-Dioxane, Water
3	43.23 ±0.17	-2.05 ±0.27	-0.32 ±0.23	1.12 ±0.22	0.93	0.17	18.97	1,2-Dichloroethane, Dichloromethane, 1,4-Dioxane
4	40.13 ±0.45	2.67 ±0.57	3.42 ±0.70	-1.51 ±0.54	0.90	0.46	12.80	Butan-2-ol, 2-Methyl propan-2-ol, Tetrahydrofuran
5	43.48 ±0.22	-2.68 ±0.62	0.12 ±0.44	1.24 ±0.29	0.92	0.22	11.16	Dichloromethane, Decan-1-ol, Ethane-1,2-diol, Hexane
6	50.80 ±2.35	-10.90 ±2.43	-6.87 ±2.06	3.08 ±0.92	0.91	0.52	8.48	1,2-Dichloroethane, 1,4-Dioxane, Ethanol, Water, Hexane, 2-Methyl propan-1-ol, Methanol
7	44.67 ±0.23	-1.83 ±0.37	0.10 ±0.38	0.11 ±0.33	0.91	0.28	11.86	Decan-1-ol, Dichloromethane, Methanol, Butan-1-ol, Tetrahydrofuran
8	44.85 ±0.82	-4.47 ±1.26	2.52 ±1.54	-0.80 ±1.00	0.90	0.83	8.81	1,2-Dichloroethane, Decan-1-ol, Dichloromethane, Ethane-1,2-diol, Ethanol, Tetrahydrofuran
9	44.64 ±0.12	-1.61 ±0.16	-0.58 ±0.16	0.80 ±0.14	0.95	0.13	33.52	Dichloromethane, Tetrahydrofuran
10	43.42 ±0.10	-0.60 ±0.14	-0.60 ±0.16	0.84 ±0.14	0.93	0.10	18.03	1,2-Dichloroethane, Water, Methanol, 2-Methyl propan-2-ol, Tetrahydrofuran

[a]Correlation coefficient; [b]Standard deviation; [c]Fisher test of significance

TABLE S-V. Results of the correlation analysis of 3-((4-substituted)phenylamino)isobenzofuran-1(3*H*)-ones according to Kamlet–Taft equation for the higher wavelength peak

Comp.	$\nu_0\times10^{-3}$ / cm^{-1}	$s\times10^{-3}$ / cm^{-1}	$b\times10^{-3}$ / cm^{-1}	$a\times10^{-3}$ / cm^{-1}	R[a]	Sd[b]	F[c]	Solvent excluded from correlation
1	43.35 ±0.21	-2.35 ±0.38	-0.23 ±0.32	1.11 ±0.27	0.91	0.21	13.28	1,2-Dichloroethane, Decan-1-ol, Dichloromethane, 1,4-Dioxane, Ethanol, Water
2	36.25 ±0.25	-2.53 ±0.35	0.02 ±0.34	0.84 ±0.28	0.94	0.26	20.43	Dichloromethane, 1,4-Dioxane, Ethane-1,2-diol, Propan-1-ol
3	33.48 ±0.27	2.89 ±0.36	0.34 ±0.38	-2.12 ±0.30	0.96	0.28	37.63	1,2-Dichloroethane, Dichloromethane, 1,4-Dioxane, Ethane-1,2-diol
4	35.30 ±1.23	-9.58 ±2.11	1.16 ±2.20	4.16 ±2.05	0.91	1.24	10.63	Decan-1-ol, Dichloromethane, 1,4-Dioxane, Ethane-1,2-diol, Water, Tetrahydrofuran
5	34.28 ±0.27	0.48 ±0.39	2.33 ±0.37	-0.97 ±0.34	0.93	0.27	13.14	1,2-Dichloroethane, Dichloromethane, 2-Methyl propan-1-ol, Methanol, Butan-1-ol, Propan-1-ol
6	33.92 ±0.41	2.32 ±0.57	1.98 ±0.61	-3.23 ±0.55	0.90	0.42	13.68	Decan-1-ol, 1,4-Dioxane, Tetrahydrofuran
7	34.76 ±0.38	0.30 ±0.48	-1.32 ±0.49	-0.98 ±0.37	0.90	0.40	16.81	Ethane-1,2-diol
8	31.34 ±0.63	-2.00 ±0.81	-0.78 ±1.11	-1.05 ±0.80	0.90	0.64	7.41	Propan-2-ol, Methanol, Butan-1-ol, Propan-1-ol, Butan-2-ol, 2-Methyl propan-2-ol, Tetrahydrofuran
9	35.70 ±0.53	0.45 ±0.83	-2.16 ±1.09	-2.78 ±0.76	0.96	0.52	9.70	Decan-1-ol, Ethanol, Water, 2-Methyl propan-1-ol, Propan-2-ol, Methanol, Butan-1-ol, Propan-1-ol, Butan-2-ol, 2-Methyl propan-2-ol
10	35.23 ±0.15	0.54 ±0.25	-0.74 ±0.23	-0.89 ±0.24	0.96	0.16	30.44	Decan-1-ol, 1,4-Dioxane, Ethane-1,2-diol, Butan-1-ol, Tetrahydrofuran

[a]Correlation coefficient; [b]Standard deviation; [c]Fisher test of significance

TABLE S-VI. Results of the correlation analysis of 3-((4-substituted)phenylamino)isobenzofuran-1(3*H*)-ones according to Catalán equation for the lower wavelength peak

Comp.	$\nu_0\times10^{-3}$ / cm^{-1}	$c\times10^{-3}$ / cm^{-1}	$d\times10^{-3}$ / cm^{-1}	$b\times10^{-3}$ / cm^{-1}	$a\times10^{-3}$ / cm^{-1}	R[a]	Sd[b]	F[c]	Solvent excluded from correlation
1	44.97 ±0.67	-2.55 ±0.99	-0.09 ±0.24	-0.85 ±0.31	-0.13 ±0.19	0.93	0.14	9.12	1,2-Dichloroethane, Water, Hexane, Methanol, 2-Methyl propan-2-ol, Tetrahydofuran
2	46.70 ±0.67	-5.57 ±0.99	-1.11 ±0.23	1.19 ±0.30	0.22 ±0.19	0.96	0.14	20.1	Decan-1-ol, Ethane-1,2-diol, Water, Methanol, Butan-1-ol, 2-Methyl propan-2-ol, Tetrahydrofuran
3	44.16 ±0.41	-1.39 ±0.59	-0.28 ±0.17	-0.64 ±0.14	-[d]	0.94	0.11	16.0	Tetrahydrofuran
4	37.78 ±1.46	3.64 ±2.09	2.86 ±0.06	-0.85 ±0.51	1.42 ±0.36	0.93	0.40	13.80	-
5	45.57 ±0.42	-3.32 ±0.63	0.13 ±0.21	-0.60 ±0.19	-0.10 ±0.14	0.95	0.09	14.40	Decan-1-ol, Dichloromethane, Water, Tetrahydrofuran
6	42.95 ±6.75	-[d]	0.14 ±5.36	-4.44 ±2.12	0.53 ±2.05	0.93	0.64	3.25	1,2-Dichloroethane, Decan-1-ol, Dichloromethane, Ethane-1,2-diol, Water, Hexane, 2-Methyl propan-1-ol, Propan-2-ol, Butan-2-ol, 2-Methyl propan-2-ol, Tetrahydrofuran
7	48.23 ±1.07	-5.91 ±1.56	0.42 ±0.48	-1.50 ±0.43	-0.36 ±0.29	0.91	0.29	8.56	Dichloromethane, Butan-1-ol, Tetrahydrofuran
8	41.0.4 ±4.94	5.60 ±7.30	-3.34 ±2.11	1.77 ±1.80	4.67 ±1.30	0.90	1.28	5.70	Propan-1-ol, Butan-2-ol, 2-Methyl propan-2-ol, Tetrahydofuran
9	46.79 ±0.18	-3.52 ±0.26	-0.84 ±0.08	0.11 ±0.07	0.13 ±0.05	0.99	0.04	124.88	1,2-Dichloroethane, 2-Methyl propan-2-ol, Tetrahydrofuran
10	43.48 ±0.36	-[d]	-0.84 ±0.15	0.25 ±0.12	-0.37 ±0.09	0.94	0.09	16.99	-

[a]Correlation coefficient; [b]Standard deviation; [c]Fisher test of significance; [d]negligible values with high standard errors

TABLE S-VII. Results of the correlation analysis of 3-((4-substituted)phenylamino)isobenzofuran-1(3*H*)-ones according to Catalán equation for the higher wavelength peak

Comp.	$\nu_0 \times 10^{-3}$ / cm^{-1}	$c \times 10^{-3}$ / cm^{-1}	$d \times 10^{-3}$ / cm^{-1}	$b \times 10^{-3}$ / cm^{-1}	$a \times 10^{-3}$ / cm^{-1}	R[a]	Sd[b]	F[c]	Solvent excluded from correlation
1	69.13 ±9.45	-38.65 ±10.27	-9.13 ±2.60	1.30 ±0.93	-2.41 ±1.26	0.96	0.25	10.49	1,2-Dichloroethane, Dichloromethane, Ethane-1,2-diol, Water, Hexane
2	40.16 ±1.63	-6.54 ±2.37	-1.61 ±0.57	0.39 ±0.52	0.99 ±0.35	0.90	0.34	8.02	Dichloromethane, Ethane-1,2-diol
3	33.91 ±1.46	-0.27 ±2.23	3.21 ±0.75	-2.94 ±0.58	-2.12 ±0.43	0.92	0.35	10.16	Decan-1-ol, Dichloromethane, Tetrahydrofuran
4	42.79 ±10.84	-12.64 ±16.81	-7.97 ±3.85	3.72 ±4.80	6.10 ±2.13	0.91	1.39	6.05	Decan-1-ol, Dichloromethane, Ethanol, Water
5	35.45 ±2.42	-1.95 ±3.78	2.13 ±0.89	-1.60 ±0.74	0.55 ±0.55	0.94	0.30	8.21	1,2-Dichloroethane, Decan-1-ol, Ethane-1,2-diol, Butan-1-ol, Tetrahydofuran, Propan-1-ol
6	34.14 ±1.09	-0.53 ±1.57	2.84 ±0.45	-3.40 ±0.54	-1.42 ±0.33	0.97	0.29	24.26	Water, 2-Methyl propan-2-ol Tetrahydrofuran
7	38.29 ±1.21	-5.42 ±1.73	0.77 ±0.50	-2.66 ±0.40	-2.04 ±0.30	0.95	0.33	22.42	-
8	37.87 ±2.17	-10.78 ±3.30	0.93 ±1.03	-3.18 ±0.72	-2.18 ±0.58	0.91	0.52	11.43	Decan-1-ol
9	50.69 ±1.16	-15.24 ±1.16	-3.99 ±0.57	-1.89 ±0.23	-2.38 ±0.27	0.99	0.17	75.75	2-Methyl propan-1-ol, Propan-2-ol, Heksan, Tetrahydrofuran
10	29.24 ±1.34	9.80 ±1.96	-1.60 ±0.58	0.14 ±0.52	-0.01 ±0.36	0.90	0.35	8.60	1.2-Dihloroethane, Tetrahydrofuran

[a]Correlation coefficient; [b]Standard deviation; [c]Fisher test of significance

TABLE S-VIII. Results of enerigies of optimized molecules by DFT/B3LYP 6-31G(d,p) method

Compound	Energy, Hartree
1	-745.3479
2	-784.6680
3	-859.8708
4	-820.5657
5	-844.5781
6	-1204.9419
7	-898.0002
8	-949.8508
9	-761.3929
10	-761.3810

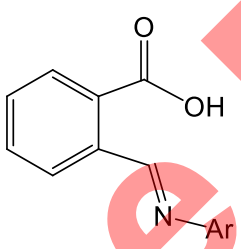

Fig. S-1. Open imine structure of synthesized compounds.

TABLE S-IX. Elements of the optimized geometries of investigated compounds, 3-((4-substituted)phenylamino)isobenzofuran-1(3H)-ones **1-10** (Å) calculated by MP2/6-31G(**) method

	C1-C7a	C1=O	C1-O2	C3-O2	C3-N	N-H	N-C1'	C1'-C2'	θ / ^{o}	μ / D
1	1.4872	1.2025	1.3727	1.4664	1.4158	1.0136	1.4141	1.4050	65.65	5.1602
2	1.4872	1.2026	1.3721	1.4675	1.4154	1.0137	1.4152	1.4046	65.64	5.0117
3	1.4871	1.2028	1.3719	1.4694	1.4149	1.0140	1.4196	1.4001	66.69	6.0281
4	1.4871	1.2027	1.3722	1.4689	1.4152	1.0141	1.4198	1.4024	66.71	6.2171
5	1.4868	1.2022	1.3738	1.4662	1.4165	1.0139	1.4136	1.4050	65.85	6.1120
6	1.4869	1.2019	1.3744	1.4643	1.4173	1.0138	1.4126	1.4048	65.29	6.3922
7	1.4869	1.2018	1.3749	1.4624	1.4178	1.0134	1.4067	1.4078	64.69	5.9823
8	1.4866	1.2011	1.3770	1.4591	1.4201	1.0133	1.4047	1.4067	64.29	9.4933
9	1.4874	1.2031	1.3713	1.4593	1.4259	1.0137	1.4048	1.4061	71.86	5.3511
10	1.4871	1.2017	1.3748	1.4611	1.4196	1.0137	1.4073	1.4031	65.23	7.0518

TABLE S-X. Molecular orbital surfaces for the HOMO and LUMO of compounds **1-10** calculated by TD-DFT/ 6-31G(d,p) method in solvent methanol

	HOMO	LUMO
1	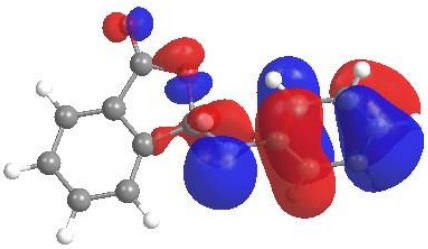	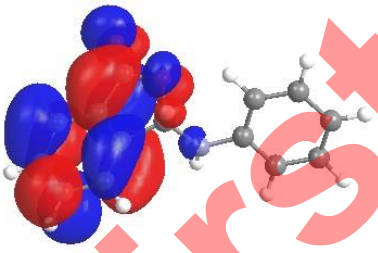
2	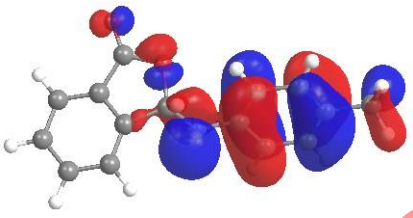	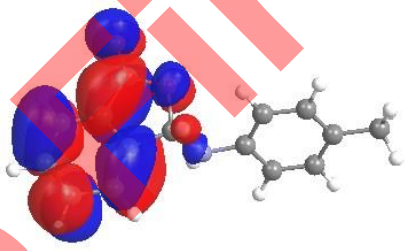
3	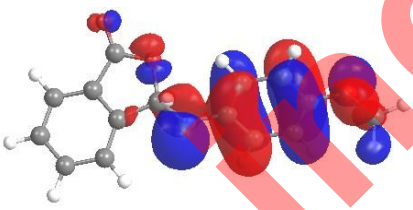	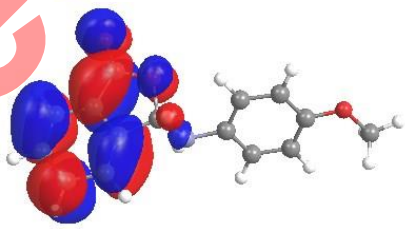
4	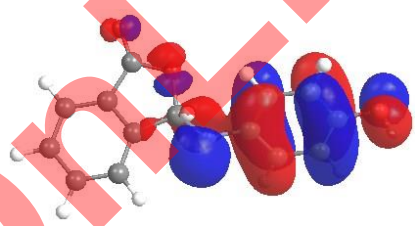	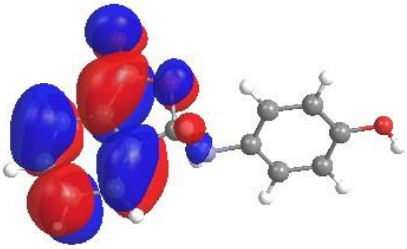
5	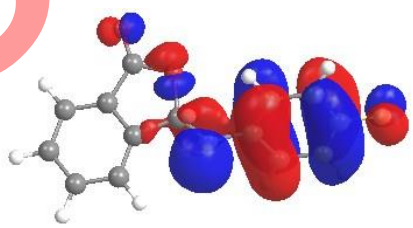	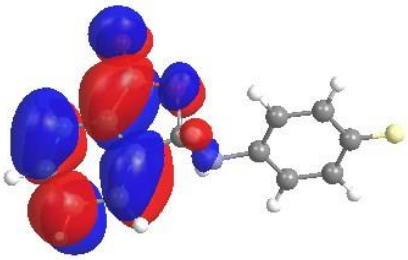

6

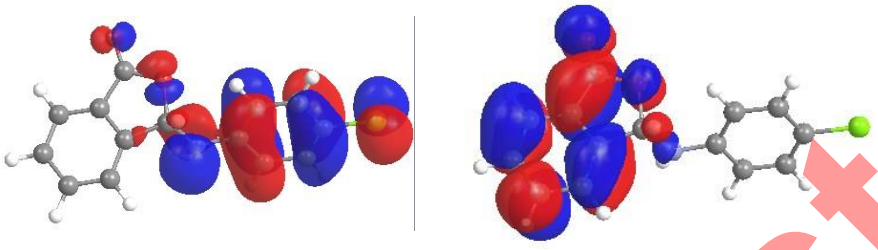

HOMO LUMO

7

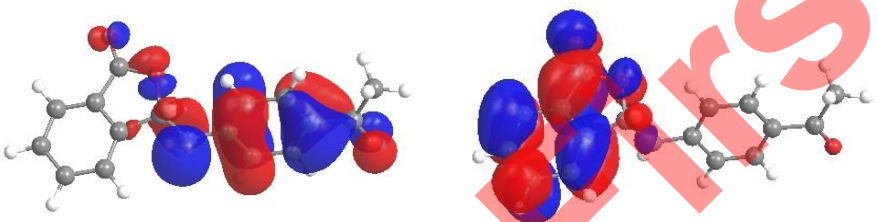

8

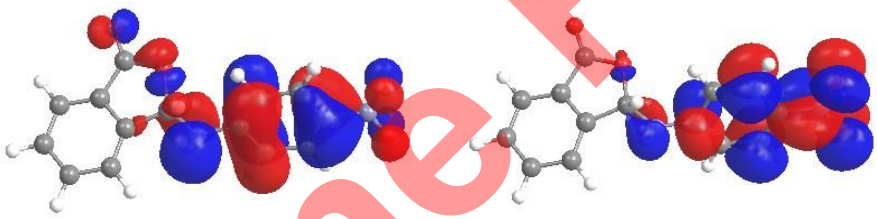

9

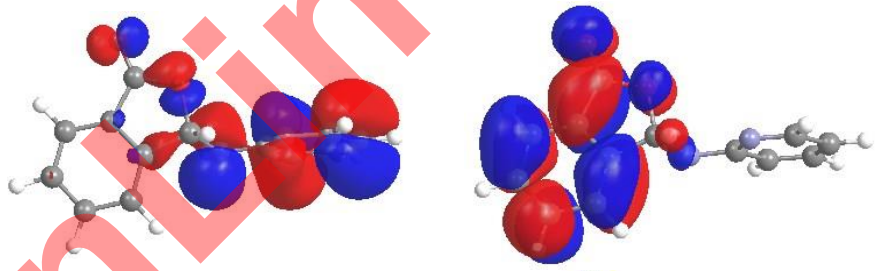

10

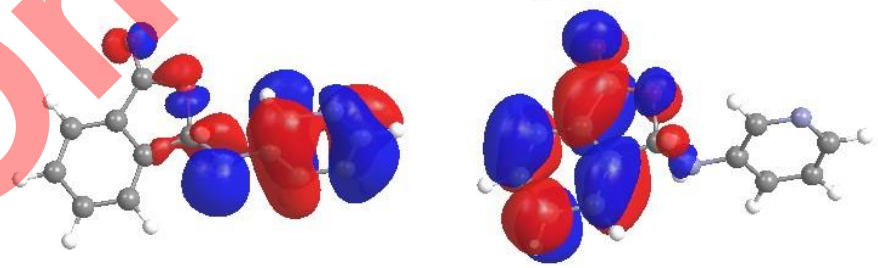

REFERENCES

1. M.J. Kamlet, J.L.M. Abboud, M.H. Abraham, R. W.Taft,. *J. Org. Chem.***48** (1983) 2877
2. Y. Marcus, *Chem. Soc. Rev.* **22** (1993) 409
3. J.Catalán, *J. Phys. Chem., B* **113** (2009) 5951.